Chapter 3

Post-START limitation of carbon-influx leads to G2 arrest and premature recruitment of the START inhibitor Whi5 in the nucleus

Athanasios Litsios and Matthias Heinemann

Molecular Systems Biology, Groningen Biomolecular Sciences and Biotechnology Institute, University of Groningen, Nijenborgh 4, 9747 AG Groningen, The Netherlands

Abstract

For decades, it has been considered that after START, the point of commitment to the mitotic cycle, yeast cells will finish their cell cycle independently of extracellular nutrient availability. However, recent studies have challenged this notion, leading to the question of how post-START cells orchestrate their on-going cell cycle processes such as bud formation and DNA replication in response to nutrient shortage. Here, using microfluidics in combination with time-lapse microscopy and single-cell reporters for cell-cycle stage and DNA synthesis, we show that glucose withdrawal leads to G2 arrest by halting bud

Author contributions: A.L. and M.H. conceived the study and wrote the manuscript. A.L. performed all experiments and analyzed the data.

growth and causing premature recruitment of the START-inhibitor Whi5 in the nucleus, but allowing for unimpeded synthesis of DNA. We show that cells with genetically-limited glycolytic flux capacity, stochastically enter G2 arrest even in the presence of glucose, suggesting that, similarly to the activation of START, a critical rate of glycolysis is essential also after START for efficient bud growth and unimpeded progression through the cell cycle. Finally, using a tandem fluorescent protein timer and an inhibitor of protein synthesis, we demonstrate that glucose flux elimination potentially elicits the G2 arrest by ceasing protein synthesis. Our results reveal different bioenergetic requirements for bud formation and DNA synthesis, and indicate an important role for glycolytic flux in post-START cell-cycle progression.

Introduction

Eukaryotic cells commit to a round of cell division after traversal though a cell cycle checkpoint that is called START in yeast, and the restriction point in mammals (Johnson and Skotheim, 2013). START is defined by the exit of the transcriptional inhibitor Whi5 from the nucleus (Doncic, Falleur-Fettig and Skotheim, 2011), activation of G1/S related transcription (Bertoli, Skotheim and de Bruin, 2013), and subsequent initiation of bud growth and DNA replication (Madden and Snyder, 1998); Bertoli, Skotheim and de Bruin, 2013). After sufficient growth of the bud and completion of DNA replication, nuclear division takes place (Lew, 2003), and the elimination of cyclin-dependent kinase (CDK) activity at mitotic exit leads eventually to the re-sequestration of Whi5 back in the nucleus (Costanzo et al., 2004), where it is retained until the commitment to a new mitotic cycle.

It has been long thought that once yeast cells have traversed through START, they will complete their cell cycle even if nutrients become later scarce. However, recent findings have shown that post-START cells are in fact sensitive to nutrient availability (Ewald et al., 2016; Laporte et al., 2011). In specific, acute glucose removal can arrest cells that have already undergone START, in a mono-nucleated state, before the completion of their cell cycle program (Ewald et al., 2016). Further, stationary phase glucose-deprived cultures were found to be composed not only of unbudded cells that have finished, or

even not initiated their cell cycle program, but also of budded cells, and thus, cells that had undergone START but did not complete cell division (Laporte et al., 2011). Such budded, post-START arrested cells were viable and did not represent fatally damaged cells (Laporte et al., 2011). These findings contrast the long-standing notion that passage through START leads to completion of the cell cycle program independent of thereafter nutrient availability. If the completion of the cell cycle program is in fact sensitive to nutrient availability, then the question arises of how cells administrate their ongoing cell-cycle processes, such as bud formation and DNA replication, once nutrients become limited.

During regular cell cycle progression, bud growth and DNA synthesis are initiated right after START, and both processes progress concomitantly until the completion of the S phase (Madden and Snyder, 1998). The coordinated onset of bud growth and DNA synthesis arises largely from Cln1 and Cln2 activity, which apart from deactivating the DNA-synthesis inhibitors Sic1 and Cdh1 (Nasmyth, 1996) also promote bud emergence and growth at the S-phase of the cell cycle (Madden and Snyder, 1998). The importance of the coordination between bud growth and DNA synthesis is highlighted by the finding that defects in bud formation lead to arrest of the cell cycle program in G2, even if DNA replication has been completed (Lew, 2003). However, the fact that DNA synthesis can proceed even if bud growth is arrested (Hereford and Hartwell, 1973) shows that while these two processes are normally coordinated, they are not coupled. Therefore, how post-START nutrient limitation impinges on the progression of each of these processes remains unclear.

Here, using microfluidics (Huberts et al., 2013; Lee et al., 2012) combined with time-lapse microscopy, and single-cell reporters for cell-cycle stage and DNA synthesis, we show that limitation in carbon influx leads to acute arrest of budding, but allows for unimpeded replication of DNA and entry and arrest to the G2 phase of the cell cycle. These events are accompanied by early re-shuttling of Whi5 in the nucleus, an event that was previously associated exclusively with entry to the G1 phase of the cell cycle. Re-establishment of favorable nutrient conditions leads to re-exit of Whi5 from the nucleus, continuation of budding, and mitosis, showing that the G2 arrest is reversible. We show

that similarly to the activation of START, a critical rate of glycolysis is also required after START for bud growth and unimpeded progression through the cell cycle. Using a tandem fluorescent protein timer (Khmelinskii et al., 2012) and a protein synthesis inhibitor, we show that the limitation of carbon influx potentially leads to the arrest of budding and the pre-mature nuclear recruitment of Whi5, by diminishing the rate of protein synthesis. Our results suggest that post-START nutrient deprivation does not lead to unconditional arrest of on-going cell cycle processes. Rather, carbon deprivation arrests post-START yeast in a G2 state, where cells have a duplicated genome, but display halted bud growth and G1-like Whi5 localization. Our findings reveal that in contrast to bud growth, DNA replication is insensitive to nutrient availability, shedding new light on how yeast cells coordinate their ongoing cell cycle processes in response to fluctuations in nutrient availability – conditions that they typically encounter in their natural niches.

Results

Post-START glucose withdrawal leads to halt of bud growth and early nuclear Whi5 recruitment

To examine how carbon deprivation affects cell cycle progression after START, we monitored the dynamics of budding in individual yeast cells that were exposed to a sudden shift from glucose-rich to glucose-free medium using a microfluidics dissection platform (Huberts et al., 2013; Lee et al., 2012). We used the localization of Whi5 to distinguish between G1 and cell-cycle committed cells, and the number of histone (Hta2) clusters (one or two) to distinguish between cells that had or had not undergone mitosis. Here, we found that upon sudden carbon withdrawal, bud growth in cells that had undergone START was almost acutely halted (Figure 1A and B) and most cells (69.4 % of 98 cells) arrested in a mono-nucleated state. The remaining fraction of cells completed their cycle, and we found that the more time that had passed between START and the moment of glucose withdrawal, the higher the probability that a cell would undergo

mitosis (denoted by the appearance of a distinct Hta2-RFP spot in the bud cell) in the absence of glucose was (Figure1 – figure supplement 1).

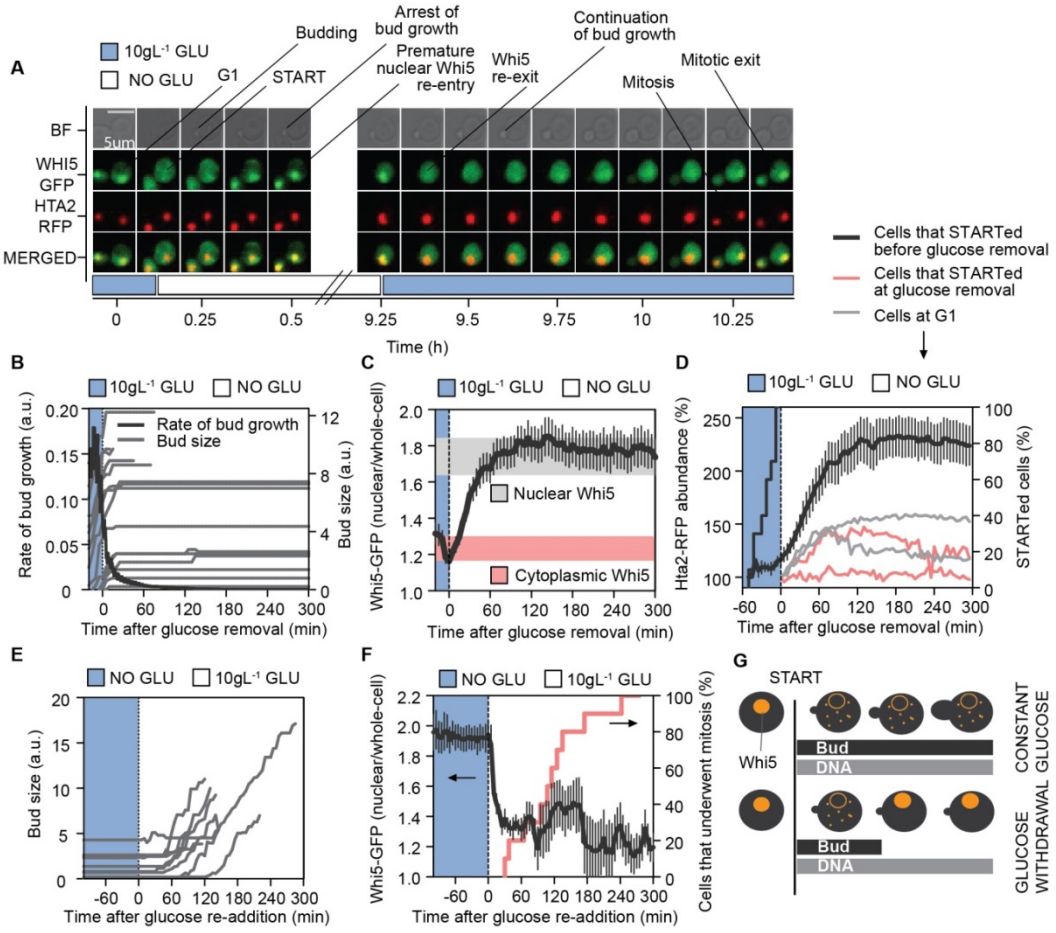

Figure 1. Glucose withdrawal after START leads to controlled G2 arrest. (**A**) Brightfield, Whi5-GFP, Hta2-RFP, and merged microscopy images of a cell that experiences glucose withdrawal after START. (**B**) Dynamics on bud growth (light-grey lines: single-cell traces of bud size; dark-grey line: mean rate of bud size increase for 17 cells), (**C**) Whi5 localization (n = 17; light-red vertical bar: lower and upper 95% CI of the Whi5-GFP nuclear-whole-cell ratio during G1 calculated from 22 single-cells growing on 10 gL^{-1} glucose; light-grey vertical bar: respective range for 19 single cells 5 min after START), and (**D**) Hta2-RFP abundance (n = 11; the dark grey line without error bars indicates the percentage of cells in the dataset that had undergone START begore the withdrawal of glucose; Light-grey and light-red indicate single-cell traces) in cells that experience glucose withdrawal after START. (**E**) Bud size (single-cell traces) and (**F**) Whi5 localization (n = 9; light-red line shows the percentage of cells in the dataset that underwent mitosis) dynamics in G2-arrested cells as a response to glucose re-addition after ≈ 9 h in carbon-free medium. In total, 85.9% out of 64 G2-arrested cells underwent mitosis after the re-addition of glucose. In all cases except the

single-cell traces, data are represented as mean ± SEM. For glucose withdrawal, the fed in the microfluidic device was switched from 10 gL^{-1} glucose minimal medium to glucose-free minimal medium. (**G**) Schematic representation of regular post-START bud growth, Whi5 localization, and DNA synthesis dynamics, and comparison with the respective dynamics after glucose withdrawal.

Strikingly, while Whi5 is thought to display nuclear localization only before cell cycle commitment, and thus, before START, we also found that upon glucose withdrawal, Whi5 was prematurely recruited back in the nucleus in nearly all cells (89.5 %) that did not complete cell division (Figure1 A and C; Figure 1 - figure supplement 2). Thus, despite the notion that the residency of Whi5 in the nucleus is restricted in the G1 phase of the cell cycle (Costanzo et al., 2004), glucose withdrawal can lead to Whi5 nuclear recruitment also at other phases of the cell cycle. These results show that carbon deprivation in cells that have undergone START, leads to complete inhibition of bud growth, premature Whi5 nuclear recruitment, and arrest of cells in a mono-nucleated state.

DNA replication progresses in post-START glucose-depleted cells

Then, we asked whether along with the pause of bud growth, these mono-nucleated cells had also inhibited DNA replication after the withdrawal of glucose. To answer this, we measured the dynamics of histone (Hta2-RFP) abundance after glucose removal in cells that had already undergone START. Because the synthesis of histones and DNA are coupled, with the inhibition of one process leading to the inhibition of the other (Nelson et al., 2002), histone abundance can be used as an estimate of DNA content in single cells (Bogenberger and Laybourn, 2008). Here, we found that despite the arrest of bud growth, cells that underwent START continued to increase their histone, and thus, DNA content after glucose withdrawal, until histone abundance was approximately doubled (Figure 1A and D). This finding suggested that these cells had managed to duplicate their genome in the complete absence of extracellular glucose.

To confirm that the duplicated histone content corresponded to duplicated DNA material, we checked whether cells which duplicated their histones after the withdrawal of glucose, could also successfully undergo mitosis. Here, we found that among the cells which had finished their cell cycle in the absence of glucose, were also cells that duplicated their histones after the withdrawal of glucose (Figure 1 – figure supplement 3A and B),

confirming that despite the arrest of bud growth, DNA replication takes place in post-START glucose-depleted cells. Thus, upon carbon deprivation, cells that have passed START and do not finish their cell cycle, complete S phase, and enter a G2 arrest characterized by duplicated genome, halted bud growth, and nuclear Whi5 localization (Figure 1G).

Replenishment of glucose leads to Whi5 re-exit, continuation of budding, and mitosis

To test whether these post-START glucose depleted cells could exit the G2-arrest and finish their cell cycle, we provided cells that were on glucose-free medium for ≈ 9 hours, again with glucose-rich medium. Here, we found that the replenishment of glucose led to a rapid exit of Whi5 from the nucleus (Figure 1A and F), continuation of budding (Figure 1 and E), and successful completion of the cell cycle (Figure 1A and F). Thus, post-START glucose-deprived cells enter a controlled G2 arrest, that is fully reversible, and whose reversibility depends on glucose availability.

A critical rate of glucose influx is required for regular cell cycle progression after START

Because in Chapter 2 we found that a critical rate of glycolysis is required for the START transition, we asked whether a critical rate of glycolysis, and not simply flux through glycolysis, is also required for proper bud growth and unimpeded completion of the cell division program. To test this, we used a yeast strain that is genetically limited to low glucose uptake rates even in the presence of high extracellular glucose levels, due to the absence of native glucose transporters and the sole expression of a chimeric hexose-transporter (HXT) gene (Otterstedt et al., 2004). Here, we found that while the vast majority of cells progressed after START smoothly through the cell cycle in the presence of glucose, at extremely rare occasions (≈5 in 1000 cell cycles) cells arrested bud growth (Figure 2A), re-sequestered Whi5 in the nucleus (Figure 2B), but unimpededly doubled their histone content (Figure 2C), entering therefore a G2 arrest. These cells could, in a stochastic fashion, re-shuttle Whi5 back to the cytoplasm, continue budding, and eventually undergo mitosis and complete their cell cycle (Figure 2A-C). Thus, low rates of glucose influx can lead to stochastic G2 arrest, suggesting that a minimum rate of glycolysis is also essential for regular cell cycle progression after START.

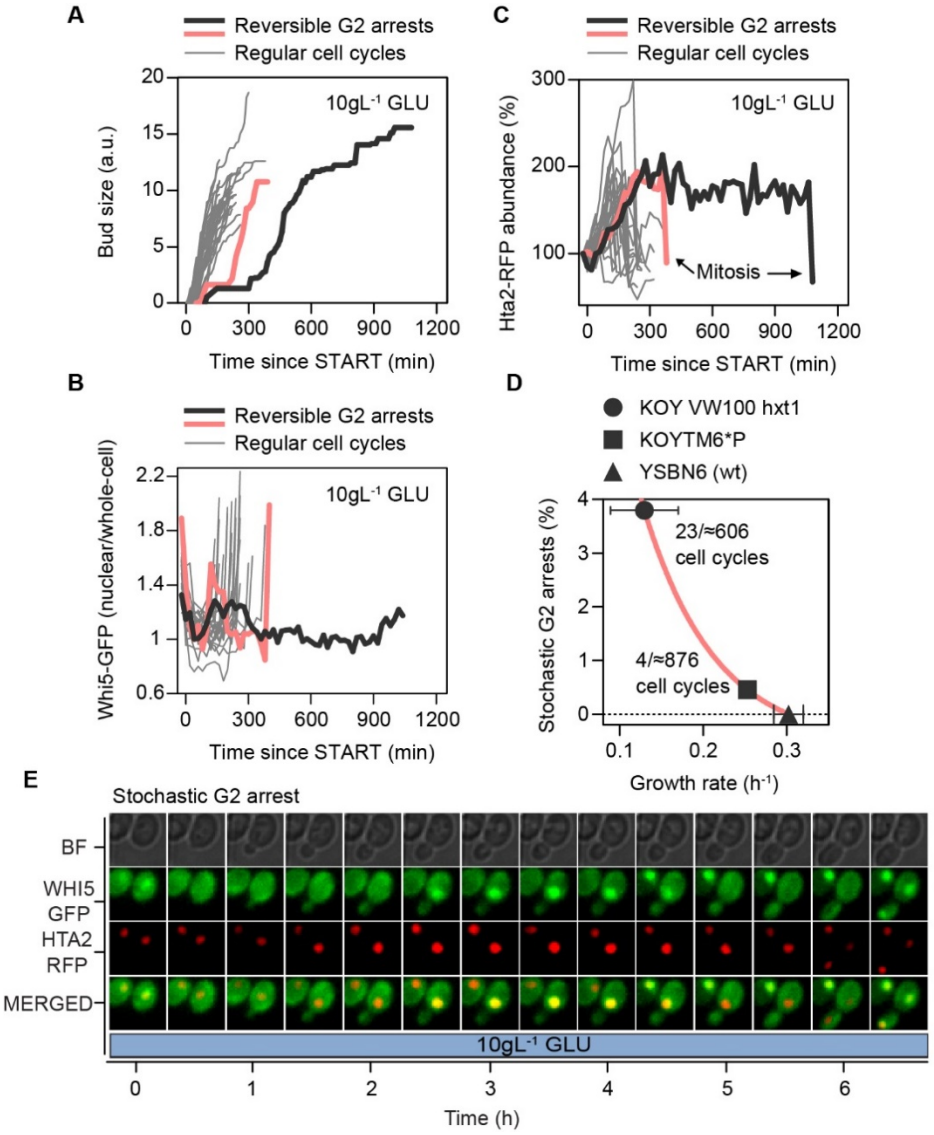

Figure 2. Low glycolytic can lead to stochastic G2 arrest in a glucose-rich environment. (**A**) Bud size, (**B**) Whi5 localization, and (**C**) Hta2-RFP abundance dynamics in stochastic, reversible G2 arrests and in regular cell cycles in a flux-limited strain (KOY TM6*P). (**D**) Occurrence of G2 arrests in glucose-rich conditions in strains with deferent steady-state glycolytic flux level. Growth rates for the KOY VW100 Hxt1 were obtained from Chapter 2. (**E**) Brightfield, Whi5-GFP, Hta2-RFP, and merged microscopy images of a cell from a flux-limited strain (KOY VW100 Hxt1), that undergoes a stochastic, reversible G2 arrest at a constant, glucose-rich environment. In all cases, cells in the microfluidics device were constantly supplemented with 10 gL^{-1} minimal medium.

To confirm that a minimum rate of glycolysis is required for regular bud growth and prevention of G2 arrest, we used a strain that lacks all known glucose transporter genes, but in which a single HXT was introduced under the regulation of an orthogonally inducible promoter (This study, Chapter 2). In glucose-rich conditions but in the absence of inducer, this strain expresses only low HXT levels and sustains a slow growth rate (This study, Chapter 2), which is even lower than the one of the single-HXT strain that was used above (Figure 2D). Here, we found that without induction, the occurrence of stochastic G2 arrests increased almost 10-fold with respect to the strain with the chimeric HXT (Figure 2D and E; Figure 2 – figure supplement 1), suggesting that that the unimpeded bud growth and progression through the cell cycle after START requires a critical rate of glycolytic flux.

Glucose deprivation can lead to G2-arrest by diminishing protein synthesis

To understand why specifically bud growth, but not DNA synthesis, was halted after glucose withdrawal, we asked whether the halted bud growth was due to the cessation of protein synthesis likely caused by the deprivation of glucose. In contrast to DNA replication, whose progression does not depend on protein synthesis, bud growth is halted immediately as a response to inhibition of protein synthesis (Hereford and Hartwell, 1973). To monitor the dynamics of protein synthesis after glucose withdrawal, we used a RFP-GFP tandem fluorescent protein timer that can report on in vivo protein turnover in single cells (Khmelinskii et al., 2012), and which we expressed by a constitutive promoter. In the absence of active degradation of the timer, increases in protein synthesis are reported by a decrease of the RFP (slow-maturing FP) to GFP (fast-maturing FP) ratio (Barry et al., 2015), while the opposite is anticipated when protein synthesis is halted. Here, we found that glucose withdrawal was indeed followed by an acute increase in the RFP-GFP ratio, indicating a cessation of protein synthesis (Figure 3A). Consistently, we found that the levels of Cln2, a cyclin that due to its instability (Salama, Hendricks and Thorner, 1994; Deshaies, Chau and Kirschner, 1995; Lanker, Valdivieso and Wittenberg, 1996) requires continuously active protein synthesis and which controls both Whi5 localization (Skotheim et al., 2008) and bud growth during early S (Madden and Snyder, 1998), rapidly dropped after glucose withdrawal (Figure 3 – figure supplement 1). Accordingly, re-addition of glucose resulted in a decrease in the RFP-GFP ratio, indicating the re-initiation of protein synthesis (Figure 3B). Importantly, bud growth following the re-addition of glucose was re-initiated only once the RFP-GFP

ratio was decreased again (Figure 3B), confirming that protein synthesis is required for bud growth.

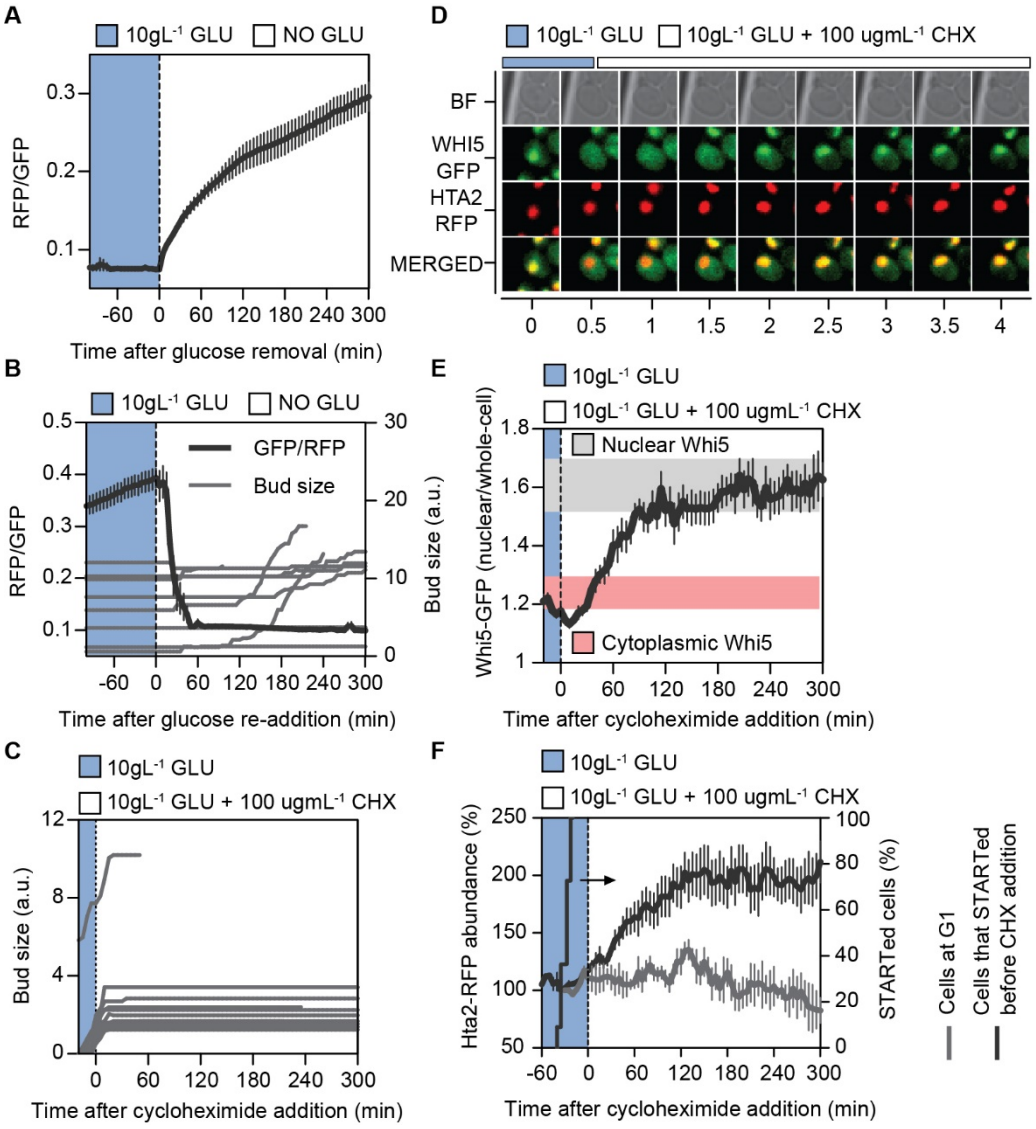

Figure 3. G2 arrested can be caused by carbon-starvation-induced cessation of protein synthesis. (**A**) RFP/GFP dynamics from a constitutively expressed tandem fluorescent protein timer as a response to glucose withdrawal (n = 16 cells). (**B**) RFP/GFP dynamics from the protein timer as a response to glucose re-addition (n = 16 cells) and respective single-cell traces of bud size dynamics for a subset of cells. (**C**) Single-cell traces of bud size, (**E**) Whi5 localization (n = 11; light-grey and light-red vertical bars that indicate nuclear and cytoplasmic Whi5 localization respectively

were estimated as described in Figure 1C from 15 and 12 single cells of the current experiment), and (**F**) Hta2-RFP abundance dynamics (n = 12 cells that have passed START at the moment of cycloheximide addition) and 3 (cells that have not passed START at the moment of the treatment); the dark grey line without error bars indicates the percentage of cells in the dataset that had undergone START begore the withdrawal of glucose) as a response to addition of the protein synthesis inhibitor cycloheximide. (**D**) Brightfield, Whi5-GFP, Hta2-RFP, and merged microscopy images of a cell that undergoes G2 arrest after the addition of cycloheximide. In all cases except the single-cell traces, data are represented as mean ± SEM. For glucose withdrawal, the fed in the microfluidic device was switched from 10 gL^{-1} glucose minimal medium to same composition medium supplemented with 100 $ugml^{-1}$ cycloheximide.

To confirm that the cessation of protein synthesis can lead to the type of G2 arrest that we observed when glucose was withdrawn, we added cycloheximide, a protein synthesis inhibitor, in cells growing constantly on glucose-rich medium. Here, we found that upon cycloheximide addition, cells halted bud growth (Figure 3C), re-sequestered Whi5 in the nucleus (Figure 3D), and duplicated their histone content (Figure 3E). The duplication of the histone content suggested first, that DNA was replicated, and second, that histone synthesis is highly resilient to perturbations of the protein synthesis machinery. Notably, the increase in Hta2-RFP fluorescence could be also due to the maturation of mRFP1 molecules in the Hta2-RFP fusion which were produced before the addition of cycloheximide, instead of de novo histone synthesis. However, the fast maturation kinetics of mRFP1 ($t_{1/2}$ = 12 min; (Jach et al., 2006) render such a scenario unlikely. Thus, the striking similarity between the G2 arrests induced by glucose withdrawal and inhibition of protein synthesis with cycloheximide, in combination with the observation that glucose withdrawal also ceases protein synthesis, suggest that glucose deprivation could potentially lead to G2 arrest through diminishing protein production.

Discussion

Although it was long thought that yeast cells can complete their cell cycle after START independently of extracellular nutrient availability, it was recently demonstrated that the majority of cells are unable to finish their cell division program upon removal of glucose (Ewald et al., 2016). One of the most crucial processes of the cell division program is the replication of the genetic material. Here, using microfluidics and single-cell analyses of cell-cycle reporters, we show that despite most post-START cells halt bud growth and do

not finish their ongoing cell-cycle program upon glucose removal, they manage to duplicate their genome and enter a state of G2-arrest (Figure 4). This state of G2-arrest is fully reversible and after the re-addition of external glucose cells resume growth and successfully undergo mitosis.

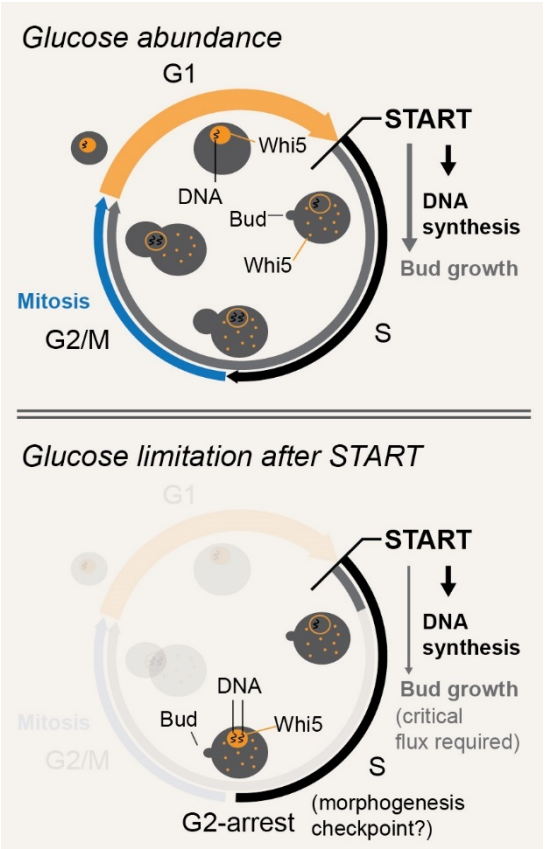

Figure 4. Scheme: Dependence of bud growth and DNA synthesis on glycolytic flux. In contrast to bud growth which requires a minimum level of glycolytic flux to progress, DNA synthesis is after its initiation almost insensitive to glycolytic flux levels. As a result, glucose withdrawal after START inhibits only bud growth but allows for DNA replication, leading cells to entry into G2-arrest. During the G2-arrest, Whi5 is prematurely localized in the nucleus.

However, the question emerges of how cells manage to complete DNA replication in the absence of extracellular carbon supply. Recent studies provided evidence that internal carbohydrate storage is liquidized during late G1 and S phases in response to CDK activity (Ewald et al., 2016; Zhao et al., 2016). Given that histones comprise only ≈ 1 % of

the proteome content (Kulak et al., 2014), and DNA comprises only ≈ 0.1 % of a cell's total mass (Sherman, 2002), DNA replication in conditions of extracellular carbon shortage could assumingly rely solely on liquidation of internal carbon pools. In fact, estimates show that the amount of carbohydrates stored in yeast is more than sufficient to synthesize DNA, but not enough for generation of new cell wall (Zhao et al., 2016). Thus, intracellular carbon storage could secure that cells finish their on-going replication of their genome and enter G2, independently of extracellular nutrient availability.

We show that the removal of glucose causes an acute cessation of protein synthesis, and also, that drug-induced inhibition of protein synthesis leads to the same type of G2-arrest even in the presence of glucose. This finding is in accordance with previous findings which suggest that bud growth is, in contrast to DNA synthesis, sensitive to inhibition of protein synthesis (Hereford and Hartwell, 1973). Moreover, we had previously found that START activation requires a critical rate of glycolysis (Chapter 2). Similarly, we show here that a sufficient rate of glycolysis is required also after START for efficient bud growth and unimpeded progression through the cell cycle. In combination, these findings could suggest that glycolytic flux facilitates bud formation, apart from providing cell wall precursors and energy, by allowing also for the sustentation of sufficient protein synthesis.

We show that upon the removal of glucose and during the G2-arrest, Whi5 is prematurely recruited in the nucleus. Interestingly, so far Whi5 has been thought to localize in the nucleus exclusively during the G1 phase of the cell cycle. In specific, CDK activity is considered to inhibit Whi5 during the START transition, leading to its shuttle from the nucleus to the cytoplasm, and elimination of CDK activity at the end of mitosis results to its re-sequestration in the nucleus (Costanzo et al., 2004). Therefore, our results suggest that the reduction of glycolytic flux leads to the premature nuclear Whi5 localization possibly by interfering with CDK activity, in consistence with the recent finding that the elimination of CDK activity (by orthogonal depletion of Cdc28) after START is sufficient to cause acute re-entry of Whi5 in the nucleus (Papagiannakis, 2017). However, whether the nuclear localization of Whi5 holds any role in the regulation of the G2-arrest, or is simply a passive outcome of the reduced glycolytic flux, remains to be elucidated.

Further, arrest in the G2 phase of the cell cycle has been previously reported to occur in yeast in the context of the morphogenesis checkpoint (Lew and Reed, 1995). While it is not clear which aspect of bud formation is monitored (Lew, 2003), the morphogenesis checkpoint delays mitosis when budding or bud growth is defective. Whether the G2 arrest that is observed in post-START cells after glucose withdrawal coincides with the morphogenesis checkpoint, is to be investigated (Figure 4).

The realization that the cell division program is after START not insensitive to the nutrient environment, opens new questions on the interplay between cell-cycle control, metabolism, and nutrient availability. Understanding this complex inter-relationship, could potentially prove useful for elucidating cell-cycle control not only in yeast, but also in more complex eukaryotic systems.

Materials and Methods

Strains and media

Yeast strains used in this study are prototrophic and of the S288C strain-background (YSBN6; YSBN16) or the CEN.PK2-1C strain-background (KOY TM6*P; KOY VW100). All strains are summarized in Table A. Minimal medium with composition (modification from Verduyn et al., 1992) per liter of 5 g of $(NH_4)_2SO_4$, 3 g of KH_2PO_4, 0.5 g of $MgSO_4 \cdot 7H_2O$, 4.5 mg of $ZnSO_4 \cdot 7H_2O$, 0.3 mg of $CoCl2 \cdot 6H_2O$, 1.0 mg of $MnCl_2 \cdot 4H_2O$, 0.3 mg of $CuSO_4 \cdot 5H_2O$, 4.5 mg of $CaCl2 \cdot 2H_2O$, 3.0 mg of $FeSO_4 \cdot 7H_2O$, 0.4 mg of $NaMoO_4 \cdot 2H_2O$, 1.0 mg of H_3BO_3, 0.1 mg of KI, 1.5 or 15 mg of EDTA, 0.05 mg of biotin, 1.0 mg of calcium pantothenate, 1.0 mg of nicotinic acid, 25 mg of inositol, 1.0 mg of pyridoxine, 0.2 mg of para-aminobenzoic acid, and 1.0 mg of thiamine, was used for all experiments. The minimal medium was further supplemented with either 10 gL^{-1} glucose or used as such for the glucose withdrawal experiments. All chemicals were purchased from Sigma-Aldrich (St. Louis, Missouri), Acros-Organics (Geel, Belgium), Formedium (Hunstanton, United Kingdom), Merck-Millipore (Billerica, Massachusetts), or Jena Bioscience (Jena, Germany).

Table A. List of yeast strains

Strain	Genotype	Source
YSBN6 (wild-type)	*MATa FY3 ho::HphMX4*	Canelas et al., 2010
YSBN6 Whi5-mGFP	YSBN6 *WHI5::mGFP-zeo*^{R}	This study
YSBN6 Whi5-mGFP Hta2-mRFP1	YSBN6 *WHI5::mGFP-zeo*^{R} *mRFP1-NatMX*	This study
YSBN16 Cln2-GFP	YSBN16 *CLN2:: eGFP-HIS3MX6*	Papagiannakis et al., 2017
YSBN6 TET-RFP-GFP	YSBN6 *ho::ptetO7-mCherry-sfGFP-KanMX4*	Huberts, 2015
KOY TM6*P	KOY.VW100P Integration into the cassette: HXT7prom-TM6*-HXT7term, ura3-52::URA3	Otterstedt et al., 2004
KOY TM6*P Hta2-RFP	KOY TM6*P *HTA2::mRFP1-NatMX*	Schmidt, 2014
KOY TM6*P Hta2-mRFP1 Whi5-mGFPa	KOY TM6*P *HTA2::mRFP1-NatMX WHI5::mGFP-zeo*^{R}	This Study
KOY VW100 Hxt1	KOY VW100P *ho::KanMX4-pINV-HXT1*	This study, Chapter 2
KOY VW100 Hxt1 Whi5-mGFP	KOY VW100P *ho::KanMX4-pINV-HXT1 WHI5::mGFP-zeo*^{R}	This study, Chapter 2
KOY VW100 Hxt1 Whi5-mGFP Hta2-mRFP1	KOY VW100P *ho::KanMX4-pINV-HXT1 WHI5::mGFP-zeo*^{R} *HTA2::mRFP1-NatMX*	This study

Strain construction

To monitor Whi5 localization and Hta2 abundance dynamics in single cells, we generated a genomic fusion of the Whi5 gene with mGFP in the YSBN6 and KOY TM6*P Hta2-RFP (Schmidt et al., 2014) strains as described in Chapter 2. Transformants were selected in the presence of zeocin (Thermo Fisher Scientific, Waltham, Massachusetts) in YPD (Formedium) (20 gL^{-1} glucose; Sigma-Aldrich) plates and correct cassette integration was confirmed by microscopically observing the expected cell-cycle dependent Whi5 localization cycles (Doncic, Falleur-Fettig and Skotheim, 2011). Then, we generated a genomic fusion of the Hta2 gene with mRFP1 in the YSBN6 Whi5-mGFP and KOY VW100 Hxt1 Whi5-mGFP strains. The integration cassette of mRFP1-NatMX with homologous overhangs to the regions upstream and downstream the stop codon of the Hta2 gene was amplified from KOY TM6*P Hta2-RFP strain using the Hta2Lin For & Rev primers (Papagiannakis et al., 2017). Transformants were selected in the presence of 100 μgmL^{-1} nourseothricin (Jena Bioscience) in YPD (20 gL^{-1} glucose for YSBN6 Whi5-mGFP Hta2-mRFP1 or 20 gL^{-1} maltose (Sigma-Aldrich) for KOY VW100 Hxt1 Whi5-

mGFP Hta2-mRFP1) plates and correct cassette integration was confirmed by microscopically observing a single bright fluorescent spot and anticipated nuclear cycles.

Determination of growth rates

For the determination of growth rate, 250-mL flasks containing 25 mL of 10 gL^{-1} glucose minimal medium were used. Media were inoculated with a single colony of YSBN6 or KOY TM6*P and cultures were incubated overnight at 30^{o}C, 300 rpm. Cultures were then diluted in 25ml fresh medium of the same initial composition and cells were allowed to attenuate exponential growth. While at exponential phase, cultures were diluted in fresh medium at a final OD_{600nm} of ≈ 0.1 and after completing at least 3 divisions, cells were further diluted in fresh medium at a final OD600nm of ≈ 0.1 before measurements were initiated. OD_{600nm} was measured by spectrophotometry.

Microfluidics

For microfluidics, cells were grown to 100-mL shake flasks containing 10ml of minimal medium supplemented with 10 gL^{-1} glucose, at 30^{o}C at a shaking speed of 300 rpm, to an OD_{600nm} of at least 0.3. Then, cells were inoculated at 10 mL fresh medium of the same composition at an OD_{600nm} of <= 0.005 and were allowed to attenuate exponential growth. Exponentially growing cells at an OD_{600nm} of 0.1-0.5 were used to load the microfluidics device. During cultivation in the microfluidic device cultivation, cells were constantly with fresh minimal medium containing 10 gL^{-1} glucose. For glucose withdrawal, the fed was switched to constant supplementation of glucose-free minimal medium pre-incubated at 30^{o}C. For the conditionally null-HXT (KOY VW100 Hxt1 Whi5-mGFP Hta2-mRFP1) strain, a different regime was followed. In specific, single colonies were used to inoculate 10 gL^{-1} maltose minimal medium. After overnight incubation, the cultures were diluted to OD_{600nm} ≈ 0.025 in 10 gL^{-1} glucose minimal medium, and were further incubated for 12 hours. Cells were then used to load the microfluidics device and were thereafter continuously supplemented with fresh 10 gL^{-1} glucose minimal medium.

Microscopy

Microscopy was performed using a microfluidics dissection platform (Huberts et al., 2013) mounted to an inverted fluorescence microscope (Eclipse Ti-E; Nikon instruments, Amsterdam, The Netherlands). The temperature was retained constant at 30^{o}C using a microscope incubator (Life Imaging Services GmbH, Basel, Switzerland). Brightfield images were recorded every 5 minutes for the wild-type strains and every 10 minutes for the HXT mutants using a 60x (CFI Plan Apo; NA = 1.4; Nikon, Tokyo, Japan) and a UV blocking filter. Fluorescent measurements were preformed using an LED-based system (pE2; CoolLED Limited, Andover, United Kingdom) and the same 60x objective, every 5 minutes for the wild-type strains and every 10 or 20 minutes for the HXT mutants. For Whi5-GFP measurements, 400 ms exposure time was used (470 nm excitation using a 470/40 nm bandpass filter and a 495 or 491 nm beam-splitter, 25 % light intensity, 525/50 nm emission filter, EM gain 3), while for Cln2-GFP measurements, exposure time was set to 500 ms (EM Gain 0). Hta2-RFP measurements were performed using 200 ms exposure time (565 nm excitation using a 560/40 or 562/40 nm excitation filter and a 585 or 593 nm beam-splitter, 20 % light intensity, 630/75 or 624/40 nm emission filter, EM gain 3). Images were captures using either an iXon Ultra 897 DU-897-U-CD0-#EX (Andor Technology Ltd) or a LucaEM R DL-604 (Andor Technology Ltd, Belfast, United Kingdom) camera. Readout speed for fluorescence imaging was set to 1 MHz. Fluctuations in axial focus during time-lapse imaging were corrected using automated hardware (PFS; Nikon).

Image and data analysis

Whole-cell fluorescence intensity measurements were performed the semi-automated ImageJ plugin BudJ (Ferrezuelo et al., 2012) was used. In all cases, acquired fluorescent intensity measurements were corrected for background autofluorescence before any further analysis, using either the Rolling Ball Background Subtraction plugin of ImageJ, or by subtracting the background intensity value estimated by BudJ (modal value of whole image). For nuclear fluorescence intensity measurements, the clustered Hta2-RFP signal was manually segmented using ImageJ. The segmented pixels were used to measure nuclear mean Hta2-RFP and Whi5-GFP fluorescence. For the calculation of histone abundance in the nucleus, an ellipse or circle was fitted at the segmented Hta2-RFP

cluster and the area of the nucleus was estimated. Hta2-RFP abundance was calculated by multiplying the mean nuclear Hta2-RFP with the nuclear area. START was identified by the sharp shuttle of Whi5-GFP from the nucleus to the cytoplasm, identified either by visual inspection or by the decrease in the ratio of Whi5-GFP nuclear to whole-cell fluorescent intensity. Bud size measurements were performed by manual segmentation of the bud using ImageJ. For the calculation of the rate of bud growth during the switch for glucose-rich to glucose-free medium, a LOWESS curve was fitted to the bud size measurements and the first derivative of the smoothed signals was calculated. Curve fitting and derivatization were performed in GraphPad Prism. The probability for a cell to undergo mitosis or display pre-mature Whi5 recruitment to the nucleus was computed using the glm function in the R package.

Acknowledgements

We would like to thank Daphne Huberts for sharing the YSBN6 TET-RFP-GFP strain. The work was funded by the Marie Curie Innovative Training Network (ITN) ISOLATE (Grant agreement no. 289995).

Competing interests

Authors declare no competing interests.

References

Barry, J., Dona, E., Gilmour, D. and Huber, W. (2015). TimerQuant: a modelling approach to tandem fluorescent timer design and data interpretation for measuring protein turnover in embryos. *Development*, 143(1), pp.174-179. doi: 10.1242/dev.125971

Bertoli, C., Skotheim, J. and de Bruin, R. (2013). Control of cell cycle transcription during G1 and S phases. *Nature Reviews Molecular Cell Biology*, 14(8), pp.518-528. doi: 10.1038/nrm3629.

Bogenberger, J. and Laybourn, P. (2008). Human T Lymphotropic Virus Type 1 protein Tax reduces histone levels. *Retrovirology*, 5(1), p.9. doi: 10.1186/1742-4690-5-9

Canelas, A., Harrison, N., Fazio, A., Zhang, J., Pitkänen, J., van den Brink, J., Bakker, B., Bogner, L., Bouwman, J., Castrillo, J., Cankorur, A., Chumnanpuen, P., Daran-Lapujade, P., Dikicioglu, D., van Eunen, K., Ewald, J., Heijnen, J., Kirdar, B., Mattila, I., Mensonides, F., Niebel, A., Penttilä, M., Pronk, J., Reuss, M., Salusjärvi, L., Sauer, U., Sherman, D., Siemann-Herzberg, M., Westerhoff, H., de Winde, J., Petranovic, D., Oliver, S., Workman, C., Zamboni, N. and Nielsen, J. (2010). Integrated multilaboratory systems biology reveals differences in protein metabolism between two reference yeast strains. *Nature Communications*, 1(9), p.145. doi:10.1038/ncomms1150

Costanzo, M., Nishikawa, J., Tang, X., Millman, J., Schub, O., Breitkreuz, K., Dewar, D., Rupes, I., Andrews, B. and Tyers, M. (2004). CDK Activity Antagonizes Whi5, an Inhibitor of G1/S Transcription in Yeast. *Cell*, 117(7), pp.899-913. doi: 10.1016/j.cell.2004.05.024

Deshaies, R.J., Chau, V. and Kirschner, M., 1995. Ubiquitination of the G1 cyclin Cln2p by a Cdc34p-dependent pathway. *The EMBO Journal*, *14*(2), pp.303-312.

Doncic, A., Falleur-Fettig, M. and Skotheim, J. (2011). Distinct Interactions Select and Maintain a Specific Cell Fate. *Molecular Cell*, 43(4), pp.528-539. doi: 10.1016/j.molcel.2011.06.025.

Ewald, J., Kuehne, A., Zamboni, N. and Skotheim, J. (2016). The Yeast Cyclin-Dependent Kinase Routes Carbon Fluxes to Fuel Cell Cycle Progression. *Molecular Cell*, 62(4), pp.532-545. doi: 10.1016/j.molcel.2016.02.017

Ferrezuelo, F., Colomina, N., Palmisano, A., Garí, E., Gallego, C., Csikász-Nagy, A. and Aldea, M. (2012). The critical size is set at a single-cell level by growth rate to attain homeostasis and adaptation. *Nature Communications*, 3, p.1012. doi: 10.1038/ncomms2015

Hereford, L. and Hartwell, L. (1973). Role of Protein Synthesis in the Replication of Yeast DNA. *Nature*, 244(135), pp.129-131. doi: 10.1038/newbio244129a0

Huberts, D., Sik Lee, S., González, J., Janssens, G., Vizcarra, I. and Heinemann, M. (2013). Construction and use of a microfluidic dissection platform for long-term imaging of cellular processes in budding yeast. *Nature Protocols*, 8(6), pp.1019-1027. doi: 10.1038/nprot.2013.060

Huberts, D., 2015. *The impact of metabolism on aging and cell size in single yeast cells* (Doctoral dissertation, University of Groningen, Groningen). Retrieved from www.rug.nl/research/portal.

Jach, G., Pesch, M., Richter, K., Frings, S. and Uhrig, J. (2006). An improved mRFP1 adds red to bimolecular fluorescence complementation. *Nature Methods*, 3(8), pp.597-600. doi: 10.1038/nmeth901

Johnson, A. and Skotheim, J. (2013). Start and the restriction point. *Current Opinion in Cell Biology*, 25(6), pp.717-723. doi: 10.1016/j.ceb.2013.07.010

Khmelinskii, A., Keller, P., Bartosik, A., Meurer, M., Barry, J., Mardin, B., Kaufmann, A., Trautmann, S., Wachsmuth, M., Pereira, G., Huber, W., Schiebel, E. and Knop, M. (2012). Tandem fluorescent protein timers for in vivo analysis of protein dynamics. *Nature Biotechnology*, 30(7), pp.708-714. doi: 10.1038/nbt.2281

Kulak, N., Pichler, G., Paron, I., Nagaraj, N. and Mann, M. (2014). Minimal, encapsulated proteomic-sample processing applied to copy-number estimation in eukaryotic cells. *Nature Methods*, 11(3), pp.319-324. doi: 10.1038/nmeth.2834

Lanker, S., Valdivieso, M. and Wittenberg, C. (1996). Rapid Degradation of the G1 Cyclin Cln2 Induced by CDK-Dependent Phosphorylation. *Science*, 271(5255), pp.1597-1601. doi: 10.1126/science.271.5255.1597

Laporte, D., Lebaudy, A., Sahin, A., Pinson, B., Ceschin, J., Daignan-Fornier, B. and Sagot, I. (2011). Metabolic status rather than cell cycle signals control quiescence entry and exit. *The Journal of Cell Biology*, 192(6), pp.949-957. doi: 10.1083/jcb.201009028

Lee, S., Vizcarra, I., Huberts, D., Lee, L. and Heinemann, M. (2012). Whole lifespan microscopic observation of budding yeast aging through a microfluidic dissection platform. *Proceedings of the National Academy of Sciences*, 109(13), pp.4916-4920. doi: 10.1073/pnas.1113505109

Lew, D. and Reed, S. (1995). A cell cycle checkpoint monitors cell morphogenesis in budding yeast. *The Journal of Cell Biology*, 129(3), pp.739-749. doi: 10.1083/jcb.129.3.739

Lew, D. (2003). The morphogenesis checkpoint: how yeast cells watch their figures. *Current Opinion in Cell Biology*, 15(6), pp.648-653.

Madden, K. and Snyder, M. (1998). Cell polarity and morphogenesis in budding yeast. *Annual Review of Microbiology*, 52(1), pp.687-744. doi: 10.1146/annurev.micro.52.1.687

Nasmyth, K. (1996). At the heart of the budding yeast cell cycle. *Trends in Genetics*, 12(10), pp.405-412. doi: 10.1016/0168-9525(96)10041-x

Nelson, D., Ye, X., Hall, C., Santos, H., Ma, T., Kao, G., Yen, T., Harper, J. and Adams, P. (2002). Coupling of DNA Synthesis and Histone Synthesis in S Phase Independent of Cyclin/cdk2 Activity. *Molecular and Cellular Biology*, 22(21), pp.7459-7472. doi: 10.1128/mcb.22.21.7459-7472.2002

Otterstedt, K., Larsson, C., Bill, R., Ståhlberg, A., Boles, E., Hohmann, S. and Gustafsson, L. (2004). Switching the mode of metabolism in the yeast Saccharomyces cerevisiae. *EMBO reports*, 5(5), pp.532-537. doi: 10.1038/sj.embor.7400132

Papagiannakis, A. (2017). *Intrinsic, periodic and tunable metabolic dynamics: a scaffold for cellular coherence* (Doctoral dissertation). Retrieved from www.rug.nl/fse.

Papagiannakis, A., Niebel, B., Wit, E. and Heinemann, M. (2017). Autonomous Metabolic Oscillations Robustly Gate the Early and Late Cell Cycle. *Molecular Cell*, 65(2), pp.285-295. doi: 10.1016/j.molcel.2016.11.018

Salama, S., Hendricks, K. and Thorner, J. (1994). G1 cyclin degradation: the PEST motif of yeast Cln2 is necessary, but not sufficient, for rapid protein turnover. *Molecular and Cellular Biology*, 14(12), pp.7953-7966. doi: 10.1128/mcb.14.12.7953

Schmidt, A.M., (2014). *Flux-signaling and flux-dependent regulation in Saccharomyces cerevisiae* (Doctoral dissertation, ETH Zürich, Zürich). Retrieved from e-collection.library.ethz.ch.

Sherman, F., 2002. Getting started with yeast. *Methods in enzymology*, *350*, pp.3-41.

Skotheim, J., Di Talia, S., Siggia, E. and Cross, F. (2008). Positive feedback of G1 cyclins ensures coherent cell cycle entry. *Nature*, 454(7202), pp.291-296. doi: 10.1038/nature07118

Zhao, G., Chen, Y., Carey, L. and Futcher, B. (2016). Cyclin-Dependent Kinase Co-Ordinates Carbohydrate Metabolism and Cell Cycle in S. cerevisiae. *Molecular Cell*, 62(4), pp.546-557. doi: 10.1016/j.molcel.2016.04.026

Supplementary material

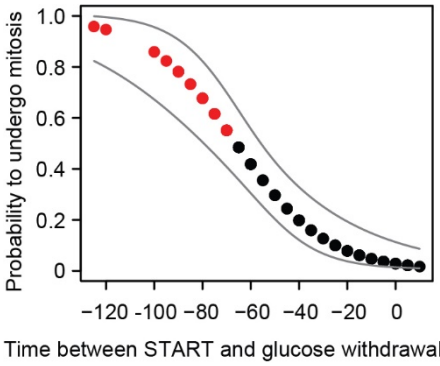

Figure 1 – figure supplement 1. Probability for a cell to undergo mitosis in the absence of glucose as a function of time passed after START at the moment of glucose withdrawal. The probability and 95% CI were calculated using logistic regression of data from 99 cells.

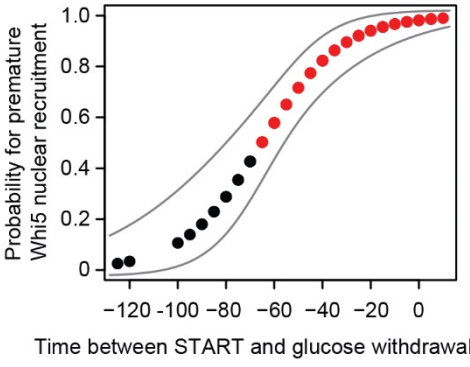

Figure 1 – figure supplement 2. Probability for a cell to prematurely recruit Whi5 in the nucleus as a function of time passed after START at the moment of glucose withdrawal. The probability and 95% CI were calculated using logistic regression of data from 92 cells.

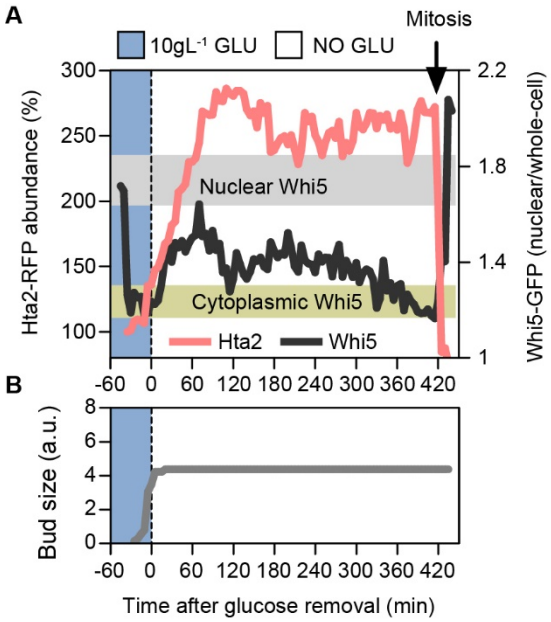

Figure 1 – figure supplement 3. Cells that duplicated their histone content after glucose-withdrawal can complete occasionally complete their cell cycle in the absence of glucose. (**A**) Hta2-RFP abundance and Whi5 localization, and (**B**) bud size dynamics in a single cell that completes its cell cycle after the switch from 10 gL^{-1} to glucose-free minimal medium. Horizontal light-grey and green bars that indicate nuclear and Whi5 localization respectively in (**A**) were estimated as described in Figure 1C.

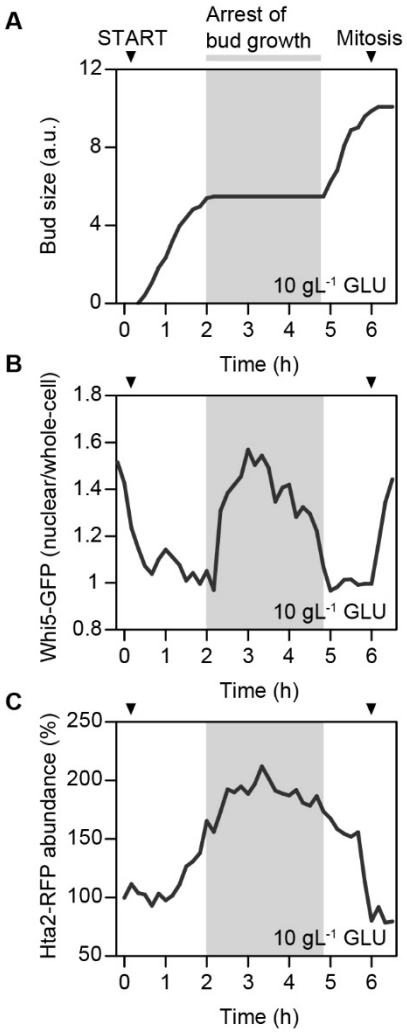

Figure 2 – figure supplement 1. Stochastic, reversible G2 arrest in a cell from a strain with genetically restricted glycolytic flux capacity. (A) Bud size, (B) Whi5 localization, and (C) Hta2-RFP abundance dynamics of the cell depicted in Figure 2E.

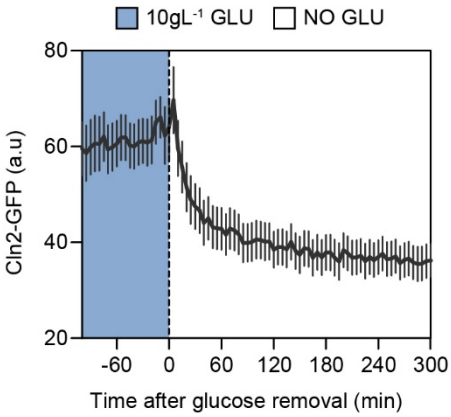

Figure 3 – figure supplement 1. CLN2-GFP dynamics as a response to glucose withdrawal. Cells in the microfluidics device were switched from 10 gL^{-1} glucose to glucose-free minimal medium. Data are represented as mean ± SEM (n = 18 cells).